A. Hussain, *et al.*: Beta-Efficiency of a Typical Gas-Flow Ionization Chamber ...
Nuclear Technology & Radiation Protection: Year 2011, Vol. 26, No. 3, pp. 193-200

193

BETA-EFFICIENCY OF A TYPICAL GAS-FLOW IONIZATION CHAMBER USING GEANT4 MONTE CARLO SIMULATIONS

by

Abid HUSSAIN, Sikander M. MIRZA, Nasir M. MIRZA*, and Muhammad T. SIDDIQUE*

Department of Physics & Applied Mathematics, Pakistan Institute of Engineering & Applied Sciences,
Nilore, Islamabad, Pakistan

GEANT4 based Monte Carlo simulations have been carried out for the determination of efficiency and conversion factors of a gas-flow ionization chamber for beta particles emitted by 86 different radioisotopes covering the average-β energy range of 5.69 keV-2.061 MeV. Good agreements were found between the GEANT4 predicted values and corresponding experimental data, as well as with EGS4 based calculations. For the reported set of β-emitters, the values of the conversion factor have been established in the range of 0.5 10^{13}-2.5 10^{13} Bqcm^{-3}/A. The computed xenon-to-air conversion factor ratios have attained the minimum value of 0.2 in the range of 0.1-1 MeV. As the radius and/or volume of the ion chamber increases, conversion factors approach a flat energy response. These simulations show a small, but significant dependence of ionization efficiency on the type of wall material.

Key words: ionization chamber, gas-flow, efficiency, GEANT4 simulations

INTRODUCTION

Ionization chambers are widely used for the measurement of radiopharmaceutical activity [1-4], external dosimetry and the assessment of radiation hazard due to inhalation of beta emitters [5, 6], as well as in the assurance of the quality of radioactivity standards [7, 8], environmental monitoring [9, 10], and radio-chronology [11].

These detectors are highly precise and yield a reproducibility of results of above 0.05% for long-lived radionuclides [12]. They are characterized by a fast response and a wide dynamic range of activity measurements. In the past, much of the research effort was centered on the calibration of ion chambers. Anderson *et al.* [13] carried out a response study of the ionization chamber to the radiation field aboard a spaceship and compared it with that of a standard Geiger-Müller detector. Yoshida *et al.* [14] used short-lived radioactive noble gases, ^{133}Xe, ^{135}Xe, and ^{41}Ar for calibration purposes. They concluded that the technique proposed can be used for a reliable estimation of the activity concentrations of gases. According to them, the influence of impurities present does not pose a serious problem.

Schrader [15] carried out a calibration of an ionization chamber based on the secondary standard measuring system for nuclear medicinal applications. The measurement of a signal-current from the re-entrant 4 γ-ionization chamber was carried out by means of a modified Townsend balance. For nineteen radionuclide and three ionization chambers used in the study, deviations of the order of 0.5% were reported. Also, the corresponding calibration quality estimator of values less than 0.2% was determined. The long-term stability of such calibrations was then tested at regular intervals using ^{137}Cs and ^{226}Rb sources. The efficiency curve for thirteen different radionuclides yielded a value of overall uncertainty better than 1.8% [16]. A revised photon efficiency curve, with a relative standard uncertainty lower than 0.01 for E_γ 65 keV, has been reported by Michotte [17], along with β-efficiency curves using seven quasi-pure beta emitters.

Fitting methods have also been used for constructing energy-dependent efficiency curves in ionization chamber applications [18], yielding differences down to a few percents from the corresponding experimental data. Michotte *et al.* [19] have developed a non-iterative approach for the determination of the ionization chamber efficiency curve and have reported that detailed calculations involving the β-spectra shape are not to be considered superfluous.

Typically, Monte Carlo based simulation techniques have been used for the theoretical estimation of the efficiency of various types of radiation detectors

---

194

A. Hussain, *et al.*: Beta-Efficiency of a Typical Gas-Flow Ionization Chamber ...
Nuclear Technology & Radiation Protection: Year 2011, Vol. 26, No. 3, pp. 193-200

[20], including ionization chambers. In most of these studies, photon-efficiency calculations have been performed. Gostley *et al.* [12] have used the GEANT code [21] for a response study of standard IG11 4 γ-ionization chambers. Amiot [22] used the PENELOPE code [23] for the determination of the calibration factor of the ionization chamber for ^{18}F, ^{99m}Tc, ^{111}In, and [123]I. Visvikis *et al.* [24] have used the GEANT4 based GATE package [25] for depth-dose profiling applications. The PENELOPE code has been employed by Kryeziu *et al.* [26] for the determination of ionization chamber calibration figures and volume correction factors for ^{90}Y, ^{125}I, ^{131}I, and [177]Lu. Simoes *et al.* [27] have utilized the MCNPX code [28] for the estimation of ionization chamber calibration coefficients for ^{18}F and [99m]Tc. By using the EGSnrc code [29], the correction factors for non-reference conditions in ion chamber photon dosimetry were also recently investigated [30].

Tompkins *et al.* [31] used bremsstrahlung measurements in ionization chambers for the determination of β-activities experimentally. Direct measurements of gaseous activities, by diffusion-in proportional counters, were carried out by Yoshida *et al.* [32] and Bielajew *et al.* [33] developed in-house parameter reduced electron step algorithm for Monte Carlo simulation of electron transport. Also, Torii [34] carried out a detailed investigation of the efficiency of the gas-flow ion chamber using the EGS4 code [35]. Reported results remained within 8% of the corresponding experimental values.

In this work, we have calculated the values of ionization chamber efficiency employing the GEANT4.9.2 code, referred to as GEANT4, hereafter. This spans the dependence of ion chamber efficiency to the range of β-energy values, radius and volume of the ion-chamber, wall material, and type of fill gas. These calculations have been performed using monoenergetic, as well as actual energy spectra, of 86 different types of β-emitters. Comparisons of the GEANT4 calculated values of efficiencies with the corresponding experimental data and with the EGS4 results are also presented in this paper.

DESCRIPTION OF THE IONIZATION CHAMBER

A commonly used detector at various nuclear facilities [34] has been selected as the standard ionization chamber for these studies. A cross-sectional view of the ion chamber, along with a detailed arrangement of its various components, is shown in fig. 1. The diameter of the cylindrical anode is 12.4 cm, its height is 15.1 cm, its effective volume 1500 cm[3]. It has a wall thickness of 0.3 cm. The cathode has a diameter of 0.5 cm and height equal to 11.2 cm. Both electrodes are made of 304-stainless steel. Normally, the chamber is filled with air at a pressure of 101.3 kPa and a temperature of 20 °C.
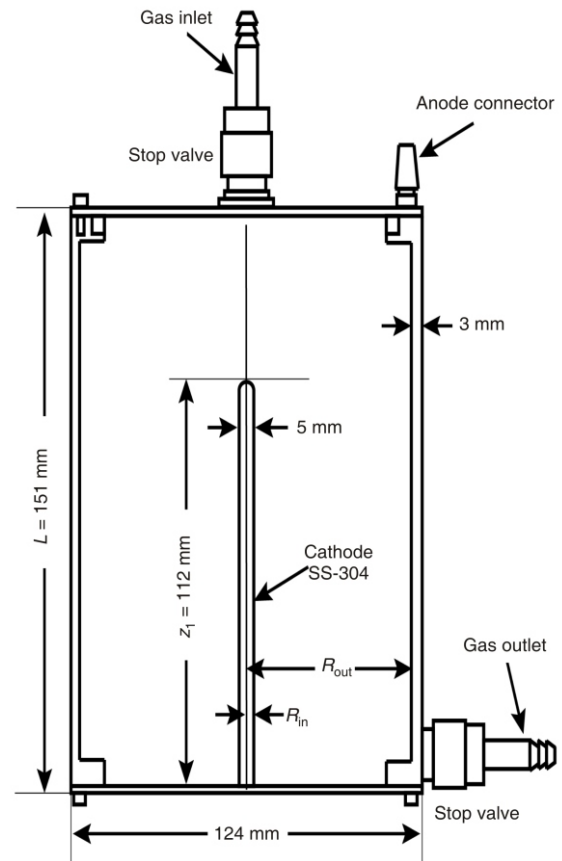

Figure 1. Schematic diagram of the ionization chamber highlighting its various components and dimensions [34]

MATERIALS AND METHODS

For efficiency calculations, the Monte Carlo based GEANT4 code has been used. The simulations start with an uniformly distributed random selection of the location of β-particle emissions from the active volume. The β-particles are emitted isotropically, in all possible random directions. This process is followed by their tracking in various regions and stops when they either leave the detector sensitive volume or their energy becomes smaller than the prescribed value of the threshold cut-off energy. In the latter case, β-particles are assumed to deposit the residual energy locally. The total energy deposition for each β-particle is calculated and this process, called sampling, is repeated a large enough number of times, so as to reduce statistical fluctuations below the prescribed limit. In these simulations, sampling of more than β-particles has been carried out for each data point averaging.

Following the steps of Samei *et al.* [36], β-spectra have been modeled by taking the product of the shape function associated with a particular transition with the Fermi function and $[(E - V_0)^2 - 1]^{1/2}$ factor; where $V_0 = 1.13 \, \alpha^2$, α is the fine structure con-

stant (1/137), and Z – the atomic number of the progeny nucleus taken as input, along with the value of the endpoint energy of each particle, percent emission, and the state and degree of transitions. The standard normalization procedure of dividing the computed probabilities with their sum over the entire energy range was applied. Furthermore, while carrying out Monte Carlo sampling, these discrete differential probabilities were converted to corresponding cumulative values.

Ionization efficiency is defined as a ratio of the measured current (I_e) to the expected current for total energy deposition (I_t). This has been calculated using the Monte Carlo summation [34] as

$$\eta = \frac{\sum_{j=1}^{J} \alpha_j \psi_j^{dep}}{\sum_{j=1}^{J} \alpha_j \psi_j^{in}} \quad (1)$$

where, $\psi_j^{dep} = \sum_{h=1}^{H} E_h^{dep}$ and $\psi_j^{in} = \sum_{h=1}^{H} E_h^{in}$ are the values of the total deposited energy and the total incident energy, respectively; with $j = 1, ..., J$, J is the total number of radiation emission modes including β decay, internal conversion and the Auger electron emission.

Since the ionization current depends on the concentration (C) of radioactive gas as in [34]

$$I_e = 1.602 \cdot 10^{-19} CVE_{ave} \frac{\eta}{W} \quad (2)$$

with V being the active volume of the ionization chamber, E_{ave} the average energy of electron per disintegration, and W – the average energy required for the ionization of the fill-gas. Therefore, the conversion factor (K), defined as the ratio of the ionization current to the concentration of radioactive gas, is given by the expression

$$K = \frac{C}{I_e} = \frac{HW}{1.602 \cdot 10^{-19} V \sum_{j=1}^{J} \alpha_j \sum_{h=1}^{H} E_h^{dep}} \quad (3)$$

where H represents the total number of incident particles used in the simulations [34]. The location of the disintegration at the cylindrical polar co-ordinates (r; θ z) has been sampled using standard relations

$$r = \begin{cases} \sqrt{\xi_1} R_{out} , & z_1 \le z \le L \\ \sqrt{\xi_1(R_{out}^2 - R_{in}^2) + R_{in}^2} , & 0 \le z \le z_1 \end{cases} \quad (4)$$

where z_1 is the height of the cathode, L – the height of the ionization chamber, and R_{in} and R_{out} are the inner and outer radii, as shown in fig. 1. The polar angle and the axial height are randomly sampled, using the equation

$$\theta = 2\pi\xi_2 \quad (5)$$

$$z = L\xi_3 \quad (6)$$

where ξ ξ and ξ_3 are uniform random numbers in the [0, 1] range.

RESULTS AND DISCUSSION

The computed values for ionization chamber efficiency of 86 different radionuclides using the GEANT4 code are listed in tab. 1, along with the corresponding values of average β-energies. The ionization chamber wall has been considered as stainless steel with air employed as the fill gas with the value of ionization energy equal to 33.97 eV per ion-pair. Comparisons of the GEANT4 computed variation of ionization chamber efficiency with energy, with the corresponding experimental data and EGS4 results, are shown in fig. 2. GEANT4 simulations have been carried out in two different instances for each radionuclide. In the first one, all β-particles have been considered to be monoenergetic, with energy equal to the corresponding average β-energy. In the second case, detailed β-spectra were employed.

From fig. 2, it is clear that monoenergetic particles tend to give overestimated values of computed efficiencies. The detailed β-spectra-based GEANT4 simulated values of efficiencies show good agreement with the corresponding experimental measurements throughout the energy range. It should be noted that the GEANT4 computed values exhibit a smaller deviation from the corresponding experimental data, especially in the medium energy range, whereas EGS4 results by Torii [34] show considerable deviations. It may also be noted that the ^{133}Xe measured value exhibits a large discrepancy with the corresponding GEANT4 computed value, which may possibly be attributed to the influence of conversion electrons, as pointed out earlier by Torii [34].

The energy-dependent variation of ionization chamber efficiency for four different fill gases has been computed using GEANT4 and the corresponding results are shown in fig. 3. As expected, with the highest Z-number, xenon has the dominating value of efficiency throughout the energy range. This is followed by argon and, then, by air mixed with methane, yielding the smallest values of efficiency. These results are based on employing detailed β-spectra in GEANT4 simulations. In all cases, the low average energy β-spectra yield larger values of ionization efficiency, since they have a higher probability of local deposition of their entire energy. The value of efficiency decreases rapidly as the average energy increases.

A good agreement is found while comparing the GEANT4 computed values of the conversion factor using detailed β-spectra with the corresponding experimental measurements, as shown in fig. 4. The computed values of the conversion factor show broad minima in the range of 0.07 MeV-0.3 MeV, whereas small variations in radionuclide concentrations yield large variations in the corresponding current. Therefore, the sensitivity of the ionization chamber towards the corresponding set of radionuclides is higher.

The dependence of the conversion factor on the radius of the ionization chamber has also been studied

196

A. Hussain, *et al.*: Beta-Efficiency of a Typical Gas-Flow Ionization Chamber ...
Nuclear Technology & Radiation Protection: Year 2011, Vol. 26, No. 3, pp. 193-200

Table 1. GEANT4 calculated values of ionization chamber efficiency for various radionuclides, for air at standard pressure and temperature (STP)

Radionuclide	$\overline{E_\beta}$ [MeV]	Efficiency	Radionuclide	$\overline{E_\beta}$ [MeV]	Efficiency
3H	0.00569	0.99241	198Au	0.313	0.09869
210Pb	0.0063	0.98873	126I	0.315	0.09732
106Ru	0.01	0.9759	43K	0.326	0.09545
63Ni	0.0172	0.94524	52Fe	0.34	0.0935
129I	0.0359	0.75033	47Ca	0.344	0.08426
95Nb	0.0434	0.73067	88Kr	0.348	0.09044
234Th	0.046	0.69276	135I	0.375	0.08006
35S	0.0488	0.68254	11C	0.386	0.07502
14C	0.0495	0.6943	99Mo	0.392	0.07654
203Hg	0.0577	0.60919	74As	0.407	0.06979
147Pm	0.062	0.57279	133I	0.409	0.07158
132Te	0.063	0.56527	81Rb	0.445	0.06531
103Ru	0.0716	0.54593	41Ar	0.464	0.06155
33P	0.0769	0.49925	13N	0.492	0.05588
45Ca	0.0772	0.481	132I	0.496	0.05503
144Ce	0.0822	0.45482	84Rb	0.527	0.04879
60Co	0.0958	0.38961	140La	0.528	0.05231
133Xe	0.1004	0.36774	24Na	0.554	0.04855
212Pb	0.101	0.37469	73Se	0.564	0.04622
59Fe	0.116	0.32255	208Tl	0.567	0.04575
95Zr	0.116	0.32157	89Sr	0.583	0.04527
82Br	0.135	0.2997	40K	0.593	0.04441
65Zn	0.143	0.28283	91Y	0.603	0.04287
141Ce	0.145	0.24603	86Rb	0.668	0.03865
28Mg	0.151	0.24617	32P	0.695	0.03618
134Cs	0.157	0.19332	15O	0.735	0.03359
47Sc	0.162	0.23353	49Sc	0.824	0.02873
192Ir	0.18	0.19697	124I	0.824	0.0288
131I	0.183	0.18541	68G	0.829	0.02737
90Sr	0.196	0.17845	234Pa^m	0.831	0.02828
58Co	0.201	0.18426	56Mn	0.832	0.02912
22Na	0.216	0.16794	49Ca	0.875	0.02692
64Cu	0.219	0.15532	90Y	0.934	0.02565
204Tl	0.238	0.14176	66Cu	1.076	0.02001
52Mn	0.242	0.14251	52Mn^m	1.172	0.01814
18F	0.25	0.13394	144Pr	1.217	0.01764
85Kr	0.251	0.12489	28Al	1.243	0.01704
62Zn	0.259	0.13077	62Cu	1.314	0.01567
140Ba	0.277	0.11623	42K	1.425	0.01550
115In^m	0.279	0.1139	106Rh	1.425	0.01437
135Xe	0.303	0.10668	82Rb	1.475	0.01310
210Bi	0.307	0.10154	38Cl	1.554	0.01479
36Cl	0.312	0.10013	88Rb	2.061	0.00923

for said 86 different radionuclides. In these simulations, the total volume of the detector has been kept at a constant of 1.5 liter. The corresponding results, as shown in fig. 5, indicate a strong dependency of the conversion factor on detector radius in the 3 cm to 5 cm range values. For larger values of detector radii, the sensitivity towards the detector radius decreases and the values of the conversion factor approach a flat limiting response.

Keeping the ratio of detector radius-to-height at a constant value of 6.2/15.1, the dependence of the conversion factor on detector volume has been studied. The corresponding GEANT4 computed variation of the conversion factor with the average-energy for detector volume in the range of 1-10 liter is shown in fig. 6. By increasing the detector volume, the energy-dependent values of the conversion factor approach a limiting flat response and detector sensitivity approaches a maximum value over nearly the entire average β-energy range.

Gas-flow ionization chambers are generally filled with air. However, methane (CH_4)- and ar-
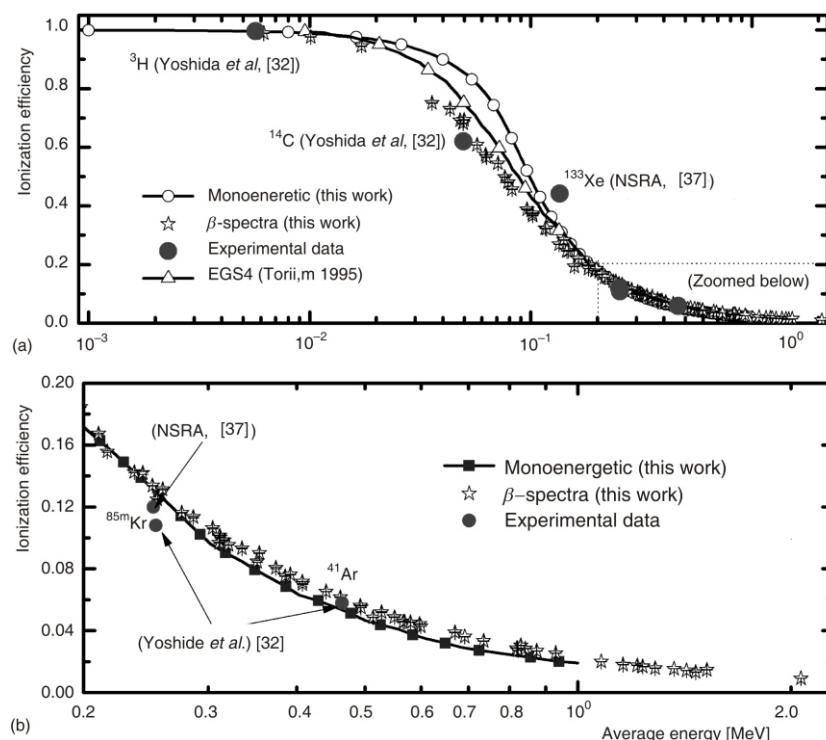
Figure 2. Variation of the standard air-filled ionization chamber efficiency with the energy for monoenergetic and continuous-particle spectra calculated by the GEANT4 code, compared with corresponding experimental data and EGS4 simulations

gon-filled chambers are also commonly used as standard for efficiency measurements [32]. In this work, GEANT4 simulations have been carried out for assessing the ratio of conversion factors of CH_4 and argon relative to that of air. The results are shown in fig. 7. The values of methane-to-air ratio of conversion factors $R_{CH_4/air}$ K_{CH_4}/K_{air} show good agreement with the corresponding experimental data by Yoshida *et al*. [32], as well as with the EGS4 results found by Torii [34]. The values for $R_{CH_4/air}$ start around 0.8 at low energies (~5 10^{-3} MeV) and rise to around 1.2 near the 2 MeV range. For average β-energies of approximately 0.1 MeV, this ratio becomes an unity

value, implying that the conversion factors for air and that of methane are identical in the said energy range.

The argon-to-air ratio of conversion factors $R_{Ar/air} = K_{Ar}/K_{air}$ also starts off with values close to 0.8 in the 5 10^{-3} MeV range and then decreases monotonically to 0.68 close to the 2 MeV range. This indicates that argon-filled ionization chambers have a smaller value of the conversion factor than the air-filled ones. These values are in good agreement with the EGS4 computed data by Torii [34]. Xenon-filled chambers have an even smaller value of the conversion factor in comparison with that of argon, with the corresponding value of the ratio of conversion factors $R_{Xe/air} = K_{Xe/Kair}$ starting off
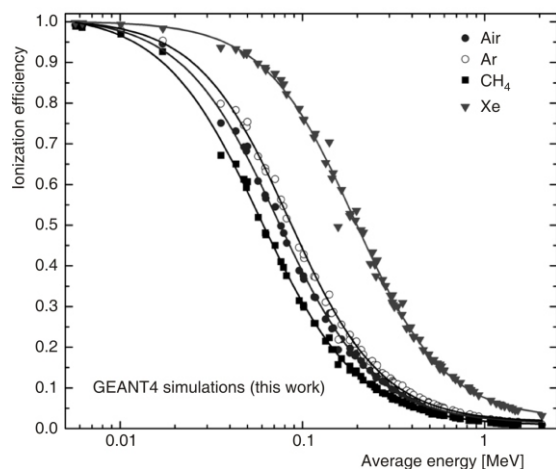

Figure 3. A continuous β spectra-based GEANT4 calculated variation of ionization chamber efficiency with the average energy for various indicated types of fill gases at standard temperatures and pressure (STP)
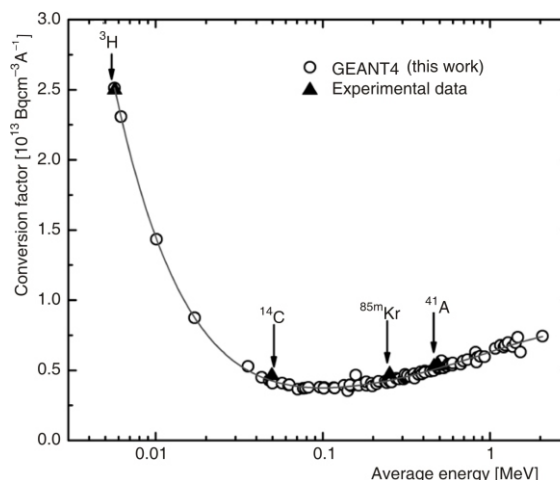

Figure 4. Comparison of the detailed spectra-based GEANT4 computed energy dependence of conversion factors with corresponding experimental measurements
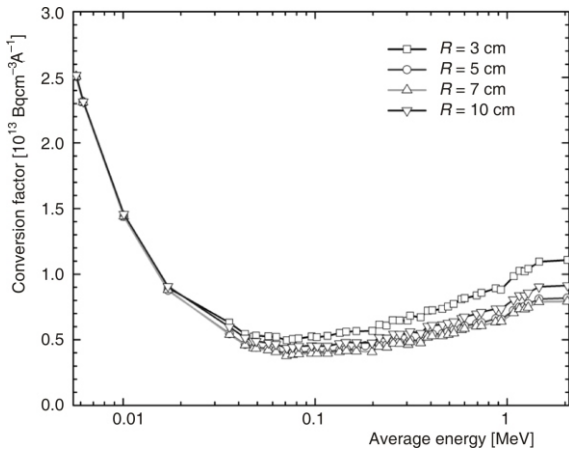
198

A. Hussain, *et al.*: Beta-Efficiency of a Typical Gas-Flow Ionization Chamber ...
Nuclear Technology & Radiation Protection: Year 2011, Vol. 26, No. 3, pp. 193-200

Figure 5. Variation of the conversion factor with average β-energy for the indicated radii of a 1.5 liter ionization chamber
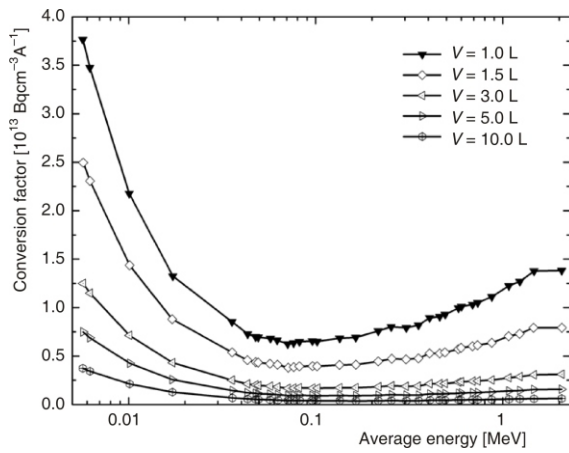

Figure 6. Variation of the conversion factor with the average β-energy for the indicated values of ionization chamber volume
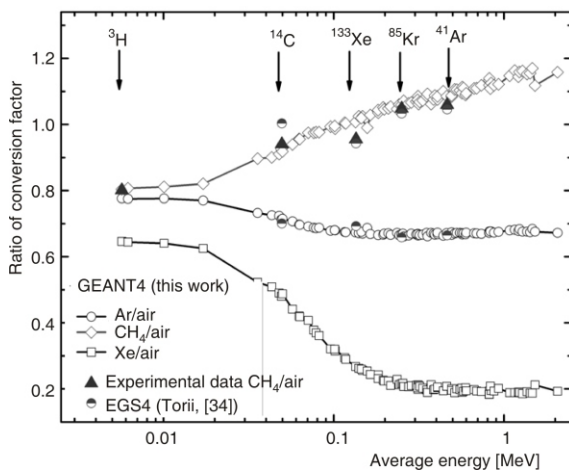

Figure 7. Variation of the indicated fill-gas-to-air conversion factor ratios with the average β-energy

from a smaller value of about 0.64 at low energies and then dropping to about 0.2 in the 2 MeV range. These results for xenon-to-air ratios are consistent with the known higher sensitivity values of xenon-filled ionization chambers.

GEANT4 simulations track β-particles even when they interact with the detector wall material. The backscatter of electrons is expected to increase the ionization efficiency of these detectors. This is clearly observed in fig. 8, when a comparison is done in the case of no-walls. The aluminum chamber and wall exhibit a higher value of ionization efficiency when compared with that of a no-walls chamber, while the stainless steel chamber exhibits the highest value. These results are in good agreement with the corresponding experimental data by Yoshida *et al.* [32]. The figure also shows that the backscatter effect is quite small, but significant enough.
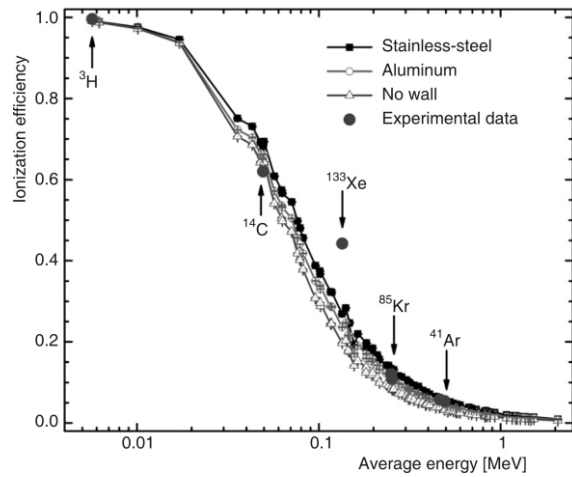

Figure 8. Comparison of the variation of efficiency with average β-energy for the indicated wall materials with the corresponding experimental data

Table 2. Values of various fill-gas parameters used in GEANT4 simulations

Fill gas	Molar mass [gmol^{-1}]	Density [mgcm^{-3}]	W [eV/ion-pair]
Air	28.96952	1.204	33.97
Xenon (Xe)	131.30	5.495	22.1
Argon (Ar)	39.948	1.6626	26.4
Methane (CH$_4$)	16.04288	0.668	27.3

CONCLUSION

In this work, the dependence of ionization chamber efficiency on β-energy, fill-gas, detector dimensions, including radius and volume, and on wall material has been studied. Detailed β-spectra have been

used in the GEANT4 based Monte Carlo simulations for tracking β-particles in the detector sensitive volume.

The following may be concluded from this work. In comparison with monoenergetic and EGS4 based calculations, the detailed β-spectra-based GEANT4 simulations yield ionization efficiency values in better agreement with the corresponding experimental data throughout the energy range.

Consistent with experimental observations, a xenon-filled ionization chamber exhibits higher values of efficiency, followed by argon-filled, air-filled, and lastly, methane-filled chamber.

The GEANT4 code based computed values for the conversion factors for 86 different radionuclides follow a smooth curve and the corresponding data show good agreement with experimental measurements.

By increasing the radius of the ionization chamber while keeping the volume constant or, by increasing the volume while keeping the height-to-radius ratio fixed, the values of the conversion factor approach a flat profile.

The GEANT4 computed ratio of conversion factors of methane to those of air (K_{CH_4}/K_{air}) shows excellent agreement with the corresponding experimental data, while the K_{Ar}/K_{air} conversion factor ratios are in good agreement with EGS4 data. Additionally, this study shows that GEANT4 based K_{Xe}/K_{air} conversion factor ratios approach the smallest values for $\overline{E_\beta}$ 0.3 MeV.

Detailed β-spectra-based GEANT4 simulations show that the energy-dependent efficiency profile has a small, but significant dependence of ionization efficiency on the type of detector wall material.

REFERENCES

[1] Perez-Mendez, V., *et al.*, Multiwire Proportion Chamber in Nuclear Medicine: Present Status and Perspective, *Int. J. Nucl. Med. Biol., 3* (1976), 1, pp. 29-30

[2] Babichev, E. A., *et al.*, Comparison of Xe and Kr Filled Ionization Chambers for Application in Digital Scanning Radiography, *Nucl. Instrum. Methods Phys. Res., A 525* (2004), 1-2, pp. 352-355

[3] Kleeven, W. J. G., Wijnhoven, G. P. J., Effect of Electrode Coating on the Response Curve of Dose Calibrators for Nuclear Medicine, *Nucl. Instrum. Methods Phys. Res., A 237* (1985), 3, pp. 604-609

[4] Pszona, S., *et al.*, A Novel Ionization Chamber for Dosimetry in Intravascular Brachytherapy, *Nucl. Instrum. Methods Phys. Res., A 537* (2005), 3, pp. 666-671

[5] Matsuyama, M., Wantanake, K., A Small Ionization Chamber Appropriate to Tritium Processing, *Fusion Engineering & Design, 18* (1991), 1, pp. 91-96

[6] Sosin, Z., Kozik, T., Majka, Z., MAGIC – Multi Anode Gas Ionization Chamber, *Nucl. Instrum. Methods Phys. Res., A 351* (1994), 2-3, pp. 383-386

[7] Parsad, K. R., *et al.*, Isotope Calibrator Ionization Chamber for Low Energy Gamma Emitters, *Appl. Radiat. Isot., 48* (1997), 7, pp. 969-971

[8] Schrader, H., Half-Life Measurements with Ionization Chambers – A Study of Systematic Effects and Results, *Appl. Radiat. Isot., 60* (2004), 2-4, pp. 317-323

[9] Dersch, R., Primary and Secondary Measurements of ^{222}Rn, *Appl, Radiat. Isot., 60* (2004), 2-4, pp. 387-390

[10] Kada, W., *et al.*, A Twin-Type Airflow Pulse Ionization Chamber for Continuous Alpha-Radioactivity in Atmosphere, *Radiat. Meas., 45* (2010), 9, pp. 1044-1048

[11] Farid, M., El-Daoushy, A. F., El-Daoushy, M. F. A. F., An Ionization Chamber and a Si-Detector for Lead-210 Chronology, *Nucl. Instrum. Meth., 188* (1981), 3, pp. 647-655

[12] Gostely, J. J., Laedermann, J. P., Simulation of the Response of the IG11 4 γ Ionization Chamber Using GEANT Monte Carlo Code, *Appl. Radiat. Isot., 52* (2000), 3, pp. 447-453

[13] Anderson, H. R., Despain, L. G., Neher, H. V., Response to Environmental and Radiation of an Ionization Chamber and Matched Geiger Tube Used on Spacecraft, *Nucl. Instrum. Meth., 47* (1967), 1, pp. 1-9

[14] Yoshida, M., *et al.*, A Calibration Technique for Gas-Flow Ionization Chambers with Short Lived Rare Gases, *Nucl. Instrum. Methods Phys. Res., A 383* (1996), 2-3, pp. 441-446

[15] Schrader, H., Calibration and Consistency of Results of an Ionization Chamber Secondary Standard Measuring System for Activity, *Appl. Radiat. Isot., 52* (2000), 3, pp. 325-334

[16] Švec, A., Schrader, H., An Ionization Chamber as a Secondary Standard for Activity, *Appl. Radiat. Isot., 52* (2000), 3, pp. 633-639

[17] Michotte, C., Efficiency Curve of the Ionization Chamber of the SIR, *Appl. Radiat. Isot., 56* (2002), 1-2, pp. 15-20

[18] Švec, A., Schrader, H., Fitting Methods for Constructing Energy-Dependent Efficiency Curves and Their Application to Ionization Chamber Measurements, *Appl. Radiat. Isot., 56* (2002), 1-2, pp. 237-243

[19] Michotte, C., *et al.*, An Approach Based on the SIR Measurement Model for Determining the Ionization Chamber Efficiency Curves, and a Study of ^{65}Zn and ^{201}Tl Photon Emission Intensities, *Appl. Radiat. Isot., 64* (2006), 10-11, pp. 1147-1155

[20] Rehman, S. U., *et al.*, GEANT4 Simulation of Photo-Peak Efficiency of Small High Purity Germanium Detectors for Nuclear Power Plant Applications, *Ann. Nucl. Energy, 38* (2011), 1, pp. 112-117

[21] Rybin, A., et al., GEAN4 – A Simulation Toolkit, *Nucl. Instrum. Methods Phys. Res., A, 506* (2003), 3, pp. 250-303

[22] Amiot, M. N., Calculation of ^{18}F, ^{99m}Tc, ^{111}In and ^{123}I Calibration Factor Using the Penelope Ionization Chamber Simulation Method, *Appl. Radiat. Isot., 60* (2004), 2-4, pp. 529-533

[23] Salvat, F., *et al.*, PENELOPE, a Code System for Monte Carlo Simulation of Electron and Photon Transport, *Proceedings*, Workshop/Training Course, OECD/NEA, Paris, November 5-7, 2001, NEA/NSC/DOC (2001) 19, ISBN:92-64-18475-9

[24] Visvikis, D., *et al.*, Use of the GATE Monte Carlo Package for Dosimetry Applications, *Nucl. Instrum. Meth. Phys. Res. A., 569* (2006), 2, pp. 335-340

[25] Santin, G., *et al.*, Evolution of the GATE Project: New Results and Developments, *Nuclear Physics B – Proceedings Supplements, 172* (2007), 1, pp. 101-103

[26] Kryeziu, D., *et al.*, Calculation of Calibration Figures and the Volume Correction Factors for ^{90}Y, ^{125}I, ^{131}I

200

A. Hussain, *et al*.: Beta-Efficiency of a Typical Gas-Flow Ionization Chamber ...
Nuclear Technology & Radiation Protection: Year 2011, Vol. 26, No. 3, pp. 193-200

and [177]Lu Radionuclide Based on Monte-Carlo Ionization Chamber Simulation, *Nucl. Instrum. Methods Phys. Res., A 580* (2007), 1, pp. 250-253

[27] Simoes, C., Caldeira, M., Oliveira, C., Comparative Study of Curiementor Ionization Chambers Using Monte Carlo Simulations, *Appl. Radiat. Isot., 68* (2010), 6, pp. 1121-1127

[28] Pelowitz, D. B., MCNPX User's Manual, Version 2.6.0, LA-CP-07-1473. LANL, 2008

[29] Kawrakow, I., *et al*., The EGSnrc Code System: Monte Carlo Simulation of Electron and Photon Transport, NRCC Report PIRS-701, NRC Canada, 2010, Available on-line: http://www.irs.inms.nrc.ca/inms/irs/EGSnrc/EGSnrc.html

[30] Wulff, J., *et al*., Investigation of Correction Factors for Non-Reference Conditions in Ion Chamber Photon Dosimetry with Monte-Carlo Simulations, *Zeitschrift für Medizinische Physik, 20* (2010), 1, pp. 25-33

[31] Tompkins, P. C., Wish, L., Burnett, W. T., Estimation of Beta-Activities from Bremsstrahlung Measurements in Ionization Chamber, *Anal. Chem., 22* (1950), 5, pp. 672-676

[32] Yoshida, M., *et al*., Direct Measurement of Gaseous Activities by Diffusion-in Long Proportional Counter

Method, *Nucl. Instrum. Methods Phys. Res., A 330* (1993), 1-2, pp. 158-164

[33] Bielajew, A. F., Rogers, D. W. O., Presta: The Parameter Reduced Electron-Step Transport Algorithm for Electron Monte Carlo Transport, *Nucl. Instrum. Methods Phys. Res. A, 18* (1986), 1-6, pp. 165-171, pp. 174-181

[34] Torii, T., Ionization Efficiency of a Gas-Flow Ion Chamber Used for Measuring Radioactive Gases by Monte Carlo Simulation, *Nucl. Instrum. Methods Phys. Res., A, 356* (1995), 2-3, pp. 255-263

[35] Nelson, W. R., Namito, Y., The EGS4 Code System: Solution of Gamma-Ray and Electron Transport Problems, SLAC PUB-5193, 1990

[36] Samei, E., *et al*., An Atlas of Selected Beta-Ray Spectra and Depth-Dose Distributions in Lithium Fluoride and Soft Tissue Generated by a Fast Monte Carlo-Based Sampling Method, *Radiat. Phys. Chem., 48* (1996), 6, pp. 719-725

[37] ***, NSRA – Nuclear Safety Research Association, Study on the Measurement of Environmental Radiation and Radioactivity, 1980, p. 125

Абид ХУСАИН, Сикандер М. МИРЗА, Насир М. МИРЗА, Мухамад Т. СИДИК

ОДРЕЂИВАЊЕ БЕТА ЕФИКАСНОСТИ ТИПИЧНЕ ЈОНИЗАЦИОНЕ ГАСНЕ КОМОРЕ ПОМОЋУ МОНТЕ КАРЛО СИМУЛАЦИЈЕ GEANT4 ПРОГРАМОМ

Ради одређивања ефикасности и конверзионих фактора јонизационе гасне коморе за бета честице, које су емитоване од 86 различитих изотопа са средњим енергијама честица од 5,69 keV до 2,061 MeV, спроведене су Монте Карло симулације засноване на GEANT4 програму. Вредности одређене GEANT4 програмом у доброј су сагласности са одговарајућим експерименталним подацима, као и са прорачунима заснованим на EGS4 коду. За означени скуп бета извора, установљене су вредности конверзионих фактора у распону $0,5 \cdot 10^{13} – 2,5 \cdot 10^{13}$ Bq/cm³A. Израчунати односи фактора конверзије ксенон-ваздух достижу минималну вредност од 0,2 у области од 0,1 MeV – 1 MeV. Уколико се радијус и запремина јонске коморе повећавају, конверзиони фактори дају раван енергетски одзив. Ове симулације показују малу али значајну зависнот ефикасности јонизације од врсте материјала зида коморе.

Кључне речи: јонизациона комора, ш̄ок ī̄аса, ефикасносш̄, GEANT4 п̄роī̄рам